Plasma Research Express

PAPER

Non-linear dynamics of electron-hole plasma induced by an electron beam

To cite this article: M S Afify *et al* 2019 *Plasma Res. Express* **1** 035010

IOP Publishing Plasma Res. Express 1 (2019) 035010 https://doi.org/10.1088/2516-1067/ab3b10

Plasma Research Express

RECEIVED
12 June 2019

REVISED
2 August 2019

ACCEPTED FOR PUBLICATION
14 August 2019

PUBLISHED
27 August 2019

PAPER

Non-linear dynamics of electron-hole plasma induced by an electron beam

M S Afify[1,4], W M Moslem[2,3] and M A Hassouba[1]

[1] Department of Physics, Faculty of Science, Benha University, Benha, Egypt
[2] Department of Physics, Faculty of Science, Port Said University, Port Said, Egypt
[3] Centre for Theoretical Physics, The British University in Egypt (BUE), El-Shorouk City, Cairo, Egypt
[4] Author to whom any correspondence should be addressed.

E-mail: mahmoud.afify@fsc.bu.edu.eg, wmmoslem@hotmail.com and hassouba@yahoo.com

Keywords: quantum fluid model, Solitons, Shock-like, and rogue waves, exchange-correlation potentials, reductive perturbation method

Abstract
This work treats the degrade of semiconductor lifetime during the pumping process. The criteria of nonlinear waves propagation that responsible for delivery the energy inside the semiconductor was determined. For this purpose, the quantum fluid model including the exchange-correlation potentials, the Bohm potential, and the degenerate pressure is employed. The reductive perturbation theory is used to reduce the basic set of quantum hydrodynamic fluid equations to Korteweg–de Vries, modified Korteweg–de Vries, and Gardner equations. When the wave carrier frequency is much smaller than the frequency of hole plasma, the non-linear rogue wave can exist and it is studied through the non-linear Schrödinger equation. This study predicts the propagation of different non-linear waves like a soliton, double layer, and rogue waves depending on the plasma and electron beam parameters. Thus, a practicable physical solution is introduced to avoid the generation of such energetic non-linear waves during the pumping process.

1. Introduction

The nanosized semiconductor devices such as quantum dots, quantum wells, and transistors had a great deal of interest where the free carrier charges of electrons/holes represent the state of plasma [1, 2]. Therefore studying the characteristics of such high-density plasmas (i.e. electrons/holes) is very important. At the absolute zero temperature, semiconductors are bad conductors but its conductivity increases with increasing the temperature of the material as more free electrons and holes could be gained [1]. The heat which results from the recombination process between electrons which located at the conduction band and holes which located at the valence band could be delivered inside the material depending on the propagation of non-linear waves such as solitons, double layer (shock-like), and rouge waves. This mechanism leads to a defect in the material because the material temperature will be raised [3, 4].

Soliton wave is a single pulse that retains its shape as it propagates and the experimental observation of such wave in semiconductors was documented by many authors, see e.g. [5] and [6]. On the other hand, the double layer consists of successive layers of net positive and net negative charge that neither propagates nor is subject to a boundary [7]. During the last few years, rogue waves are considered one of the most serious phenomena in nature [8]. It is characterized by a short lifetime and a sudden generation with high energy where the first observable was in mid-ocean and coasted water as it causes damages in petroleum platforms and nuclear power plants that constructed on the edge of the ocean [9]. Moreover, the existence of this wave had been observed experimentally in different fields of physics such as fiber optics [10, 11], Bose-Einstein condensates [12], and plasma physics [13]. An insight of theoretical non-linear theory, the modulational instability could be used to study the mechanism of rogue waves propagation.

A theoretical study of the rogue wave generation in plasma physics was performed by many authors (see e.g. [14–16]). Recently, Yahia *et al* [17] studied the propagation of freak waves in GaN semiconductors. Moreover, they clarify the existence range for the rogue wave. Also, El-Bedwehy [18] discussed the generation of a rogue wave in GaAs semiconductors including factors that can lead to rogue wave generation. In case of nanosized semiconductors, the quantum fluid model is convenient as the plasma number density is very high and so the de Broglie wavelength is larger than the mean interparticle distance of plasma component [19]. Although, several works discussed the quantum effects (i.e. Fermi degenerate pressure, Bohm potential, and exchange-correlation potentials) in quantum plasma, it still ambiguous and needs further studies. More details about quantum plasma can be found in [20–28]. In fact, for a system of ultrahigh density and low temperature, the exchange-correlation effects of electrons/holes should be important [29–31]. In a quantum system, the density-functional theory (DFT) for the ground states is the general techniques to study the exchange-correlation potentials rather than the many-electron Schrödinger equation which becomes very complicated [32, 33]. The (DFT) depends on the electrostatic density at each point in space and has a lot of applications in modern technologies [34]. Moreover, the time-independent DFT is the popular approach for the excited states, rather than the time-dependent DFT (TDDFT) approach which has challenging problems, where [35, 36] gives more details about time-independent DFT and TDDFT approaches. The time-independent DFT potentials used here had been introduced by Brey *et al* [37] in solid-state physics which became familiar in plasma physics after introducing the time-independent DFT potentials into the quantum hydrodynamical (QHD) model by Crouseilles *et al* [38]. Recently, Choudhury *et al* [39] discussed more details about an exchange-correlation potentials in semiconductor plasma. This work aimed to find a physical solution to the degrades of the semiconductors lifetime that exposure to an electron beam. Furthermore, to the best of our knowledge, no attempt has been made to investigate the generation of freak waves during the pumping process using an electron beam. Therefore, to avoid the harms of the propagation of such non-linear waves, we focus our study on the excitation parameters (i.e. the density, velocity, and temperature of the electron beam) of the GaAs to lower non-linearity. For that purpose, the quantum fluid model had been applied where the basic equations were reduced to the K-dV, mK-dV, and Gardner evolution equations using the reductive perturbation techniques where the propagation of soliton and shock-like waves had been investigated. Moreover, the Gardner equation was transformed into a non-linear Schrödinger (NLS) equation. Therefore the instability regions that may be responsible for the heating of semiconductors during the pumping process could be determined, hence this is a facility to overcome this challenge.

2. The theoretical model

Consider a plasma system consisting of free electrons and holes in a nano bulk size semiconductor where the holes have the same role as ions in the gaseous plasma. This system is pumped by an electron beam with an initial velocity u_{b0} number density n_{b0}. Moreover, the charge neutrality condition at equilibrium is $n_{e0} + n_{b0} = n_{h0}$, where n_{e0} and n_{h0} are the equilibrium number densities of electrons and holes respectively. The quantum hydrodynamic fluid model that including the quantum effects arising through the exchange-correlation potentials and Bohm potential [40] had been employed. Owing to the high density of the electron-hole plasma, the Fermi degenerate pressure had been used for the electron-hole momentum equations. This is because at high density the quantum effects resulting from the Fermi–Dirac statistics are dominant with respect to the quantum contributions arising from the wave nature of the carrier charges. On the other hand, the thermal pressure had been considered for the classical electron beam momentum equation. Therefore, the total set of the normalized quantum fluid model is

$$\frac{\partial n_e}{\partial t} + \frac{\partial}{\partial x}(n_e u_e) = 0, \tag{1}$$

$$\frac{\partial u_e}{\partial t} + u_e\frac{\partial u_e}{\partial x} - \frac{\partial \varphi}{\partial x} + \frac{\partial V_{xce}}{\partial x} + \beta_1 n_e^{-1/3}\frac{\partial n_e}{\partial x} + \frac{1}{3}H_e^2\frac{\partial}{\partial x}\left(\frac{\frac{\partial^2}{\partial x^2}\sqrt{n_e}}{\sqrt{n_e}}\right) = 0, \tag{2}$$

$$\frac{\partial n_h}{\partial t} + \frac{\partial}{\partial x}(n_h u_h) = 0, \tag{3}$$

$$\frac{\partial u_h}{\partial t} + u_h\frac{\partial u_h}{\partial x} + M\frac{\partial \varphi}{\partial x} + M\frac{\partial V_{xch}}{\partial x} + \beta_2 n_h^{-1/3}\frac{\partial n_h}{\partial x} + \frac{1}{3}H_h^2\frac{\partial}{\partial x}\left(\frac{\frac{\partial^2}{\partial x^2}\sqrt{n_h}}{\sqrt{n_h}}\right) = 0. \tag{4}$$

$$\frac{\partial n_b}{\partial t} + \frac{\partial}{\partial x}(n_b u_b) = 0, \tag{5}$$

$$\frac{\partial u_b}{\partial t} + u_b\frac{\partial u_b}{\partial x} - \mu\frac{\partial \varphi}{\partial x} + 3\mu\sigma n_b\frac{\partial n_b}{\partial x} = 0. \tag{6}$$

The Poisson's equation for the latter system of equations (1)–(6) is

$$\frac{\partial^2\varphi}{\partial x^2} = n_e + \nu n_b - \rho n_h, \tag{7}$$

where m_e^* and m_h^* are the effective masses of electrons and holes respectively and $n_e\,(u_e)$, $n_h\,(u_h)$, and $n_b\,(u_b)$ are the density (velocity) of the electrons, holes, and electron beam respectively, ε_0 is the permittivity, and e is the magnitude of electron charge. The last equations (1)–(7) and variables are normalized to the plasma frequency, Debye length, and Fermi velocity. Also, n_e, n_h, and n_b are normalized by the unperturbed number densities n_{e0}, n_{h0}, and n_{b0} of electrons, holes, and electron beam respectively. The time is normalized by the inverse of plasma frequency $\omega_{pe}^{-1} = \left(\frac{\varepsilon_0 m_e^*}{e^2 n_{e0}}\right)^{-1/2}$, while space is normalized by the Fermi Debye radius $\lambda_{DFe} = \left(\frac{k_B T_{Fe}\varepsilon_0}{e^2 n_{e0}}\right)^{1/2}$. The velocity u and the potential φ are normalized by the Fermi electron speed $V_{Fe} = \left(\frac{k_B T_{Fe}}{m_e^*}\right)^{1/2}$ and $\frac{k_B T_{Fe}}{e}$ respectively. Moreover, $M = m_e^*/m_h^*$ is the electron-to-hole effective mass ratio, $\nu = (n_{b0}/n_{e0})$ and $\rho = (n_{h0}/n_{e0})$ are the unperturbed electron beam number density and unperturbed hole number density to the unperturbed electron number density respectively, $\beta_1 = \frac{2}{3}$, $\beta_2 = (2/3)n_{e0}^{-2/3}n_{h0}^{2/3}/(M)$, $H_e = (\hbar\omega_{pe}/\sqrt{2}K_B T_{Fe})$, $H_h = (\hbar\omega_{pe}/\sqrt{2}K_B T_{Fe})M$, $\mu = (m_e^*/m_b)$, and $\sigma = (T_b/T_{Fe})$. The $V_{xce,h}$ is the exchange-correlation potentials of electrons and holes that are given by $V_{xce,h} = -\frac{(0.985e^2\sqrt[3]{n_{e,h}}\sqrt[3]{n_{e0,h0}})}{\in}\left(1 + \frac{0.034}{a_{Be,h}^*\sqrt[3]{n_{e,h}}\sqrt[3]{n_{e0,h0}}}\ln(1 + 18.37a_{Be,h}^*\sqrt[3]{n_{e,h}}\sqrt[3]{n_{e0,h0}})\right)$, where $a_B^* = \frac{\in\hbar^2}{e^2 m_{e,h}^*}$ is the effective Bohr radius and $\in$ is the dielectric constant. The degenerate pressure [41] of the charge carriers electrons/holes that used in equations (2) and (4) is given by $P_{e,h} = K_{e,h}n_{e,h}^{5/3}$, where $K_{e,h} = \frac{3}{5}(\pi/3)^{1/3}\pi\hbar^2/m_{e,h}^*$, $\hbar$ is the Planck constant divided by 2π. The classical pressure had been used in equation (6), $P_b \propto n_b^3$. Quite recently, considerable attention had been paid to the locality of Bohm potential where a prefactor $\gamma = (D-2)/3D$ should be added in front of the Bohm potential depending on the system dimensionality D [42]. Therefore, for the 1D system, the factor $-1/3$ had been added in front of the fourth terms in equations (2) and (4)

3. Derivation of Evolution equations

The propagation of non-linear acoustic waves can be investigated using the reductive perturbation technique [43]. As a result of this method, we introduced the following stretching of space-time variables [44]

$$\xi = \varepsilon^{1/2}(x - \lambda t) \quad \text{and} \quad \tau = \varepsilon^{3/2}t, \tag{8}$$

where ε is a small quantity less than one and λ is the phase velocity which can be determined from the compatibility condition. We expanded the physical parameters in equations (1)–(7) as a power series in ε about their equilibrium values as

$$\begin{Bmatrix} n_e \\ u_e \\ n_b \\ u_b \\ n_h \\ u_h \\ \varphi \end{Bmatrix} = \begin{Bmatrix} 1 \\ 0 \\ 1 \\ u_{b0} \\ 1 \\ 0 \\ 0 \end{Bmatrix} + \sum_{j=1}^{\infty}\varepsilon^j \begin{Bmatrix} n_e^j \\ u_e^j \\ n_b^j \\ u_b^j \\ n_h^j \\ u_h^j \\ \varphi^j \end{Bmatrix} \tag{9}$$

Substituting from equations (8) and (9) into the equations (1)–(6), then the lowest order in ε yields

$$\begin{aligned} n_{e1} &= \frac{\varphi_1}{\gamma_1 - \lambda^2}, \quad u_{e1} = \frac{\lambda\varphi_1}{\gamma_1 - \lambda^2}, \\ n_{h1} &= \frac{-M\varphi_1}{\gamma_2 - \lambda^2}, \quad u_{h1} = \frac{-M\lambda\varphi_1}{\gamma_2 - \lambda^2}, \\ n_{b1} &= \frac{\mu\varphi_1}{3\mu\sigma - (u_{b0} - \lambda)^2}, \quad u_{b1} = \frac{\mu(u_{b0} - \lambda)\varphi_1}{3\mu\sigma - (u_{b0} - \lambda)^2}. \end{aligned} \tag{10}$$

The constants γ_1 and γ_2 are given in appendix A.

The first order of Poisson's equation (7) gives the following compatibility condition

$$\frac{1}{\gamma_1 - \lambda^2} + \frac{\mu\nu}{3\mu\sigma - (u_{b0} - \lambda)^2} + \frac{\rho M}{\gamma_2 - \lambda^2} = 0. \tag{11}$$

Taking into account the next-order in ε, we obtained the following equation

$$\lambda\frac{\partial n_{e2}}{\partial\xi}-\frac{\partial u_{e2}}{\partial\xi}=\frac{\partial n_{e1}}{\partial\tau}+\frac{\partial}{\partial\xi}(u_{e1}n_{e1}),\tag{12}$$

$$\begin{aligned}&\frac{\partial u_{e1}}{\partial\tau}-\gamma_{4e}\gamma_{5e}^{2}n_{e1}\frac{\partial n_{e1}}{\partial\xi}-\frac{2}{3}\gamma_{4e}\gamma_{5e}n_{e1}\frac{\partial n_{e1}}{\partial\xi}-\frac{2}{9}\gamma_{3e}n_{e1}\frac{\partial n_{e1}}{\partial\xi}+u_{e1}\frac{\partial u_{e1}}{\partial\xi}\\&+\gamma_{4e}\gamma_{5e}\frac{\partial n_{e2}}{\partial\xi}+\frac{1}{3}\gamma_{3e}\frac{\partial n_{e2}}{\partial\xi}-\lambda\frac{\partial u_{e2}}{\partial\xi}-\frac{\partial\varphi_2}{\partial\xi}+\frac{1}{3}\beta_1 n_{e1}\frac{\partial n_{e1}}{\partial\xi}-\beta_1\frac{\partial n_{e2}}{\partial\xi}+\frac{1}{6}H_e^2\frac{\partial^3 n_{e1}}{\partial\xi^3}=0,\end{aligned}\tag{13}$$

$$\lambda\frac{\partial n_{h2}}{\partial\xi}-\frac{\partial u_{h2}}{\partial\xi}=\frac{\partial n_{h1}}{\partial\tau}+\frac{\partial}{\partial\xi}(u_{h1}n_{h1}),\tag{14}$$

$$\begin{aligned}&\frac{\partial u_{h1}}{\partial\tau}-M\gamma_{4h}\gamma_{5h}^{2}n_{h1}\frac{\partial n_{h1}}{\partial\xi}-\frac{2}{3}M\gamma_{4h}\gamma_{5h}n_{h1}\frac{\partial n_{h1}}{\partial\xi}-\frac{2}{9}M\gamma_{3h}n_{h1}\frac{\partial n_{h1}}{\partial\xi}+\frac{1}{3}\beta_2 n_{h1}\frac{\partial n_{h1}}{\partial\xi}\\&-\beta_2\frac{\partial n_{h2}}{\partial\xi}+u_{h1}\frac{\partial u_{h1}}{\partial\xi}+M\gamma_{4h}\gamma_{5h}\frac{\partial n_{h2}}{\partial\xi}+M\frac{1}{3}\gamma_{3h}\frac{\partial n_{h2}}{\partial\xi}-\lambda\frac{\partial u_{h2}}{\partial\xi}+M\frac{\partial\varphi_2}{\partial\xi}+\frac{1}{6}H_h^2\frac{\partial^3 n_{h1}}{\partial\xi^3}=0,\end{aligned}\tag{15}$$

$$(\lambda-u_{b0})\frac{\partial n_{b2}}{\partial\xi}-\frac{\partial u_{b2}}{\partial\xi}=\frac{\partial n_{b1}}{\partial\tau}+\frac{\partial}{\partial\xi}(u_{b1}n_{b1}),\tag{16}$$

$$\frac{\partial u_{b1}}{\partial\tau}+(u_{b0}-\lambda)\frac{\partial u_{b2}}{\partial\xi}+u_{b1}\frac{\partial u_{b1}}{\partial\xi}=\mu\frac{\partial\varphi_2}{\partial\xi}-3\mu\sigma\frac{\partial n_{b2}}{\partial\xi}-3\mu\sigma n_{b1}\frac{\partial n_{b1}}{\partial\xi}.\tag{17}$$

The constants $\gamma_{3e,h}$, $\gamma_{4e,h}$, and $\gamma_{5e,h}$ are given by Appendix A. Using equations (10) and (11) to solve equations (12)–(17) for φ_1, we obtain the final evolution equation as

$$\frac{\partial}{\partial\tau}\varphi_1+AB\varphi_1\frac{\partial}{\partial\xi}\varphi_1+AD\frac{\partial^3}{\partial\xi^3}\varphi_1=0,\tag{18}$$

where the coefficients A, D, and the non-linear coefficient B are presented in the appendix A. Equation (18) is the well known Korteweg–de Vries (KdV) equation, that describes the propagation of the non-linear acoustic waves during the interaction between the semiconductor charge carriers (electrons/holes) and the electron beam. The coefficients A, B, and D can provide us with the probability to exist non-linear acoustic waves or not. It is known that both A and D are positive, while the coefficient B may be either positive or negative owing to the change of the plasma parameters. Our attention is given to the propagation of non-linear acoustic waves in GaAs semiconductor owing to its importance in modern technology. It is known that the specimen of GaAs is characterized by high carrier mobility and direct energy gap, thus it admits high photonic quantum yield in a nano-sized material. As a result of that, it has several applications in high-speed electronics such as solar cells, laser diodes, and microwave frequency integrated circuits [1]. However, the pumping process is considered a source of the non-linearity of the GaAs medium, as it raises the material temperature which reduces the lifetime of GaAs. Researches on the pumping process of semiconductors have become popular and take considerable attention from many authors. Coelho *et al* [45] discussed the GaAs defects during the pumping process using a low energy electron beam. Also, Archila *et al* [46] documented that energy can travel through the lattice as wave packets, then it delivers energy to produce defects. Recently Tunhuma *et al* [47] studied an experimental solution which shows the mechanisms responsible for the damage of GaAs. In the following analyze, we give theoretical investigation to the defect formation in GaAs during the excitation process using a classical electron beam. Here are the typical values of GaAs physical parameters $n_0 = 4.7 \times 10^{22}$ m^{-3}, $m_e^* = .067m_e$, and $m_h^* = .5m_e$ [21, 48]. Figure 1 represented the polarity of the non-linear coefficient B, where the positive and negative values of B depends on the electron beam velocity u_{b0} and temperature ratio σ. It is clear that the positive region is dominant for a wide range of beam velocity u_{b0} and temperature σ, where the yellow region refers to the positive values of B, while the green region refers to the negative values of B. The dashed lines refer to the values of $B = 0$ which mean the non-linear coefficient B vanishes and so the non-linear term of equation (18) disappears. Therefore, the non-linear behavior of the system cannot be described by the KdV equation. The perturbation of electrons and holes provides the plasma with different non-linear waves. Moreover, the soliton wave is an important type that carries energy for a long distance without dissipation, and so it becomes a gate of defects. Therefore, the pumping process should be controlled in order to minimize such non-linear waves to avoid the harmful noises. To get the soliton solution for equation (18), we introduce a new transformed coordinate X with respect to a frame moving with velocity U

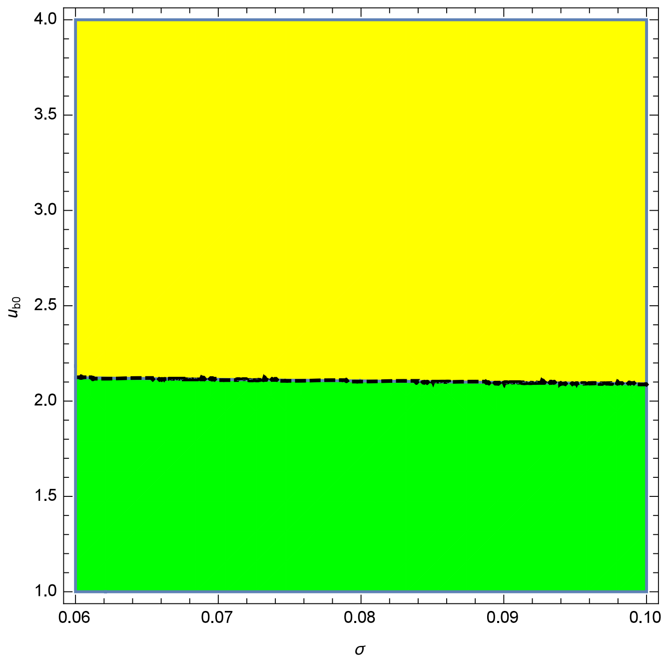

Figure 1. The contour plot of the electron beam stream velocity u_{b0} against the electron beam temperature ratio σ for nanosized GaAs with parameters $n_0 = 4.7 \times 10^{22}\ \mathrm{m}^{-3}$, $m_e^* = 0.067 m_e$, $m_h^* = 0.5 m_e$. Here, $\nu = 0.002$ and $V_g = 0.01$.

$$X = \xi - U\tau, \tag{19}$$

into equation (18) and taking into account the boundary conditions $\varphi \to 0$ and $\frac{d\varphi}{dX} \to 0$ at $|X| \to \infty$, we have

$$\varphi_1 = \varphi_0\ \mathrm{sech}^2\left(\frac{X}{w_1}\right), \tag{20}$$

where X is the transformed coordinate with respect to a frame moving with velocity U, $w_1 = \left(\frac{4AD}{U}\right)^{\frac{1}{2}}$ is the wave width, and $\varphi_0 = \frac{3U}{AB}$ is the solitary pulse amplitude.

We can now proceed analogously to the effect of electron beam parameters on the acoustic soliton profile and examine how the electron beam changes both the amplitude and width pulse. As can be seen from figure 2(a), increasing the electron beam streaming velocity leads to increasing the energy of the soliton pulse. Furthermore, increasing the density of the electron beam leads to increasing the amount of heat gained by the soliton wave as illustrated in figure 2(b). Therefore, both the electron beam velocity u_{b0} and density ν had a significant effect on the soliton amplitude and width.

It is interesting to investigate the propagation of non-linear waves at the critical density, thus we derive the following evolution equation which describes the non-linear waves at $B = 0$.

$$\frac{\partial \varphi_1}{\partial \tau} + AC\ \varphi_1^2 \frac{\partial \varphi_1}{\partial \xi} + A\ D \frac{\partial^3 \varphi_1}{\partial \xi^3} = 0, \tag{21}$$

where equation (21) is called the modified (K-dV) equation and the non-linear coefficient $C \neq 0$ at the critical values of B. Furthermore, it is convenient to combine equations (18) with (19) in order to have a new general evolution equation that represents the system in the vicinity of $B \sim O(\varepsilon)$ and at the critical values of the non-linear term B to yield

$$\frac{\partial \varphi_1}{\partial \tau} + (AB\varphi_1 + AC\ \varphi_1^2) \frac{\partial \varphi_1}{\partial \xi} + AD \frac{\partial^3 \varphi_1}{\partial \xi^3} = 0. \tag{22}$$

Equation (22) is called the Gardner equation [49]. More details about the derivation of equations (21) and (22) are given in appendix B.

Now, it is useful to study the double-layer solution of equation (22) under the condition that the non-linear coefficient C is always negative. The double layer (DLs) solution is known as a shock-like solution and it consists of two positive and negative layers of equal or different plasma density [50]. These charges may lose their energy to the plasma medium causing an increase in the temperature.

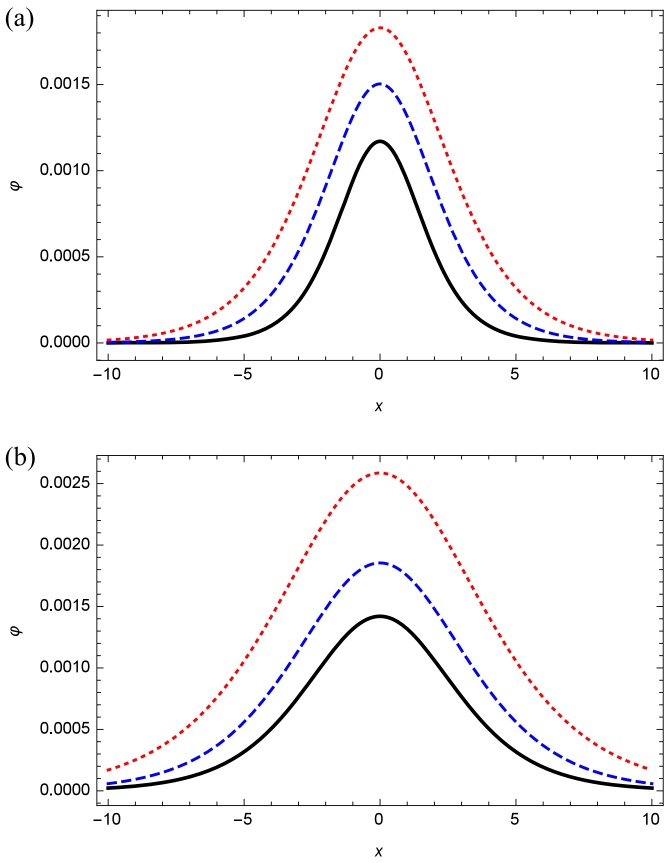

Figure 2. Positive acoustic solitary pulses, (a) variation of electric potential φ with electron beam velocity u_{b0} for GaAs with parameters $\sigma = 0.06$, $u_{b0} = 2.5$ (solid curve), $u_{b0} = 2.7$ (dashed curve), and $u_{b0} = 2.9$ (dotted curve) and (b) the electric potential φ against the electron beam density ν for GaAs with parameters $\sigma = 0.06$, $u_{b0} = 3.5$, $\nu = 0.001$ (solid curve), $\nu = 0.001\ 3$ (dashed curve), and $\nu = 0.0018$ (dotted curve). Here, the plasma parameters are the same as in figure 1.

Taking into account the traveling-wave transformation (19) and substituting into equation (22) then integrating the result equation considering the boundary conditions $\varphi \to 0$ and $\frac{d\varphi}{dX} = \frac{d^2\varphi}{dX^2} \to 0$ at $|X| \to \pm\infty$, we obtain

$$\left(\frac{\partial \varphi_1}{\partial X}\right)^2 + V(\varphi) = 0, \tag{23}$$

where $V(\varphi)$ is a Sagdeev potential and given by the following equation

$$V(\varphi) = \frac{-U}{AD}\varphi_1^2 + \frac{B}{3D}\varphi_1^3 + \frac{C}{6D}\varphi_1^4. \tag{24}$$

The next conditions should be satisfied by Sagdeev potential for the DLs structure

$$V(\varphi) = 0 \text{ at } \varphi = 0 \text{ and } \varphi = \varphi_m, \tag{25}$$

$$V'(\varphi) = 0 \quad \text{at} \quad \varphi = 0 \quad \text{and} \quad \varphi = \varphi_m, \tag{26}$$

$$V''(\varphi) = 0 \quad \text{at} \quad \varphi = 0 \quad \text{and} \quad \varphi = \varphi_m. \tag{27}$$

Using the boundary conditions (25) and (26) into equation (24), we get

$$U = \left(\frac{-AB^2}{6C}\right) \quad \text{and} \quad \varphi_{m1} = \frac{-B}{C}. \tag{28}$$

Taking into account U and φ_{m1} from equations (28) into (24), we have

$$V(\varphi) = \frac{C}{12D}\varphi_1^2(\varphi_{m1} - \varphi_1)^2. \tag{29}$$

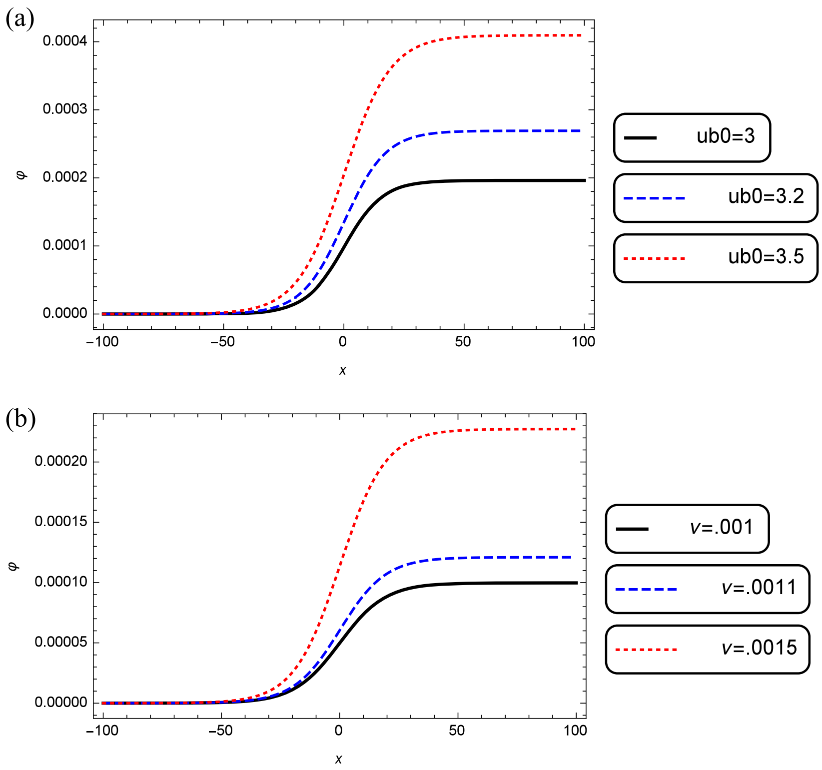

Figure 3. Variation of the shock-like profiles with (a) electron beam stream velocity u_{b0} where $\nu = 0.002$ and (b) electron beam density ν where $u_{b0} = 3.5$. Taking the plasma parameters as the same as in figure 1.

Substituting equations (29) into (22) and after some algebraic manipulations, we get the DLs solution as

$$\varphi_1 = \frac{\varphi_{m1}}{2}\left[1 + \tanh\left(\varphi_{m1}\sqrt{\frac{-C}{24D}}X\right)\right]. \tag{30}$$

For a clear insight to the plasma bulk in case of the interaction between the electron beam and the electron/hole plasma, we have outlined the profile of the shock-like pulses against the electron beam parameters in figure 3. According to figure 3(a), it is obvious that the DLs has a relatively small amplitude about 0.00016 when $u_{b0} = 3$. Further slight increasing in u_{b0} leads to provide the DLs amplitude 4 times where for $u_{b0} = 3.5$ the amplitude growing to 0.00042. Reaching the double-layer amplitude to this value by slightly increase in u_{b0} means that the shock-like wave gain more energy, hence this excess of energy may raise the material temperature and cause defects in the semiconductors. The double layer profile had the same behavior with respect to changing the electron beam density. Consider figure 3(b), which plots the double layer potential against the density of electron beam ν, for a very slight increase in the electron beam density leads to a sudden increase in the shock-like amplitude. It is known that the wave amplitude is the main measurement to the wave energy where taller waves cause a high potential difference, that accelerate the charged particles to high speed. Therefore, if the electron beam parameters (i.e streaming velocity u_{b0} and density ν) are controlled successfully, then the lifetime of semiconductors may be increased by avoiding such growing of noises during the pumping process.

4. The Evolution equation of rogue wave

It is interesting to study the propagation of rogue wave during the excitation process of nano-sized semiconductor which may be a source of heat that reduces the lifetime of the semiconductor. For that purpose, we need to derive the NLS equation that provides us with more information about the stability (instability) of the non-linear wave packet that gives rise to the propagation of the rogue wave. Moreover, the NLS equation can be derived directly using the derivative expansion method where it is valid for all wavenumbers. On the other hand, the derivation of the NLS equation from the Gardner equation (22) is valid for small wave number only. Owing to the electron beam streaming velocity, the direct derivation of the NLS equation using the Krylov-Bogoliubov-Mitropolsky method [51] is not possible. Therefore, it is convenient to transform the Gardner equation (22) into the corresponding NLS equation and further details about this procedure can be found in [52, 53]. Now, we introduce the following wave function φ to obtain the NLS equation [54]

$$\varphi(\xi, \tau) = \sum_{n=1}^{\infty} \epsilon^n \sum_{l=-n}^{n} \varphi_{l,n}(X, T) \exp il(k\,\xi - \omega\,\tau), \tag{31}$$

where k is the carrier wave number, ω is the wave frequency, and the coordinates X and T are given by

$$X = \epsilon(\xi - V_g\,\tau) \quad \text{and} \quad T = \epsilon^2 \tau. \tag{32}$$

It is interesting to note that, there are two different time scales where the first one represents the carrier waves with fast scales ξ, τ, and phase velocity v_g. Furthermore, the second one refers to the envelope wave packet with slow scales X, T, and group velocity V_g. In fact, the wave function $\varphi(\xi, \tau)$ which given by equation (31) should be real, thus the condition $\varphi_{l,n} = \varphi_{l,n}^*$ must be satisfied where the asterisk refers to the complex conjugate. Taking into account equation (32), the derivation that appearing in equation (22) can be replaced by the following derivative operators

$$\frac{\partial}{\partial \xi} \longrightarrow \frac{\partial}{\partial \xi} + \epsilon \frac{\partial}{\partial X} \quad \text{and} \quad \frac{\partial}{\partial \tau} \longrightarrow \frac{\partial}{\partial \tau} - \epsilon V_g \frac{\partial}{\partial X} + \epsilon^2 \frac{\partial}{\partial T}. \tag{33}$$

Substituting from equations (31) and (33) into (22), the following linear dispersion relation can be obtained from the first harmonic ($l = 1$) of the first-order approximation ($n = 1$)

$$\omega = -ADk^3. \tag{34}$$

Moreover, the group velocity can be derived from the first harmonic ($l = 1$) of the second-order approximation ($n = 2$) to give

$$V_g = 3ADk^2. \tag{35}$$

Finally, the NLS equation results from the first harmonic ($l = 1$) of the third-order approximation ($n = 3$) so we have

$$i\,\frac{\partial \Phi}{\partial T} + P\,\frac{\partial^2 \Phi}{\partial X^2} + Q\,\,|\Phi|^2 \Phi = 0. \tag{36}$$

where $P = 6ADk$ is the dispersion coefficient, $Q = \frac{B^2}{6kD} - kAC$ is the non-linear coefficient and $\Phi \equiv \varphi_{3,1}$. Equation (36) had different mathematical solutions where the most important setting is the rational solution given by the following equation [55]. The latter type is located on a nonzero background and localized both in the X and T directions and the general convenient form to express the NLS equation (36) is

$$\Phi_j(X, \check{T}) = \sqrt{\frac{P}{Q}} \left[(-1)^j + \frac{G_j(X, \check{T}) + i\check{T} H_j(X, \check{T})}{F_j(X, \check{T})} \right] \exp(i\check{T}), \tag{37}$$

where $\check{T} = PT$ and $F_j(X, \check{T})$ has no real zeros where j is the order of the solution. The functions $G_j(X, \check{T})$ and $H_j(X, \check{T})$ are polynomials in the variables X and $\check{T}$. Actually, the solution (37) of the NLS equation (36) indicated that an amount of the wave energy is concentrated into a small region due to the non-linear behavior of the medium.

It is important to take into account the sign of the ratio P/Q to know whether the changing of wave amplitude is modulational stable or not. The positive values of P/Q refer to the wave amplitude is modulational unstable, while the negative values of P/Q refer to the wave amplitude grows modulational stable. It is surprising that the modulated wave may give rise to a ponderomotive force that can trap particles causing a local depression in density called a caviton. Moreover, the non-linear waves trapped in this cavity are resonances at the group velocity then array an isolated structure called an envelope soliton or rogue wave. The latter is corresponding to the condition that $P/Q > 0$ while for $P/Q < 0$ we have dark soliton [56]. According to figure 4, the positive values of P/Q which represented by the yellow region are dominant where the green region refers to the negative values of P/Q. Therefore the $(u_{b0} - \sigma)$ plan is a serious tool to predict the propagation of the rogue wave during the pumping process. Moreover, increasing both the electron beam stream velocity u_{b0} and the wavenumber k leads to an increase in the amplitude of the rogue wave as represented by figures 5(a) and (b). It is clear that a slight increase of the electron beam velocity and the wave number leads to a sudden increase in the rogue wave amplitude and width. Also, this indicates that the short wavelength acoustic waves are modulational unstable and the corresponding solution of the NLS equation gives rise to a bright soliton. From this, we deduce that the electron beam velocity and the wave number plays an important role in increasing the rogue wave energy where the wave amplitude represents the wave energy. For more description about the rogue wave profile, we investigated the effect of Bohm potential on the rogue wave profile. As is clear from figure 6, the absence of the tunneling effect leads to a decrease in the rogue wave amplitude and makes pulses narrower. We concluded that the tunneling effect may be a source of heat as the electrons can penetrate the rogue wave trapping center and then raising the substance resistance by exchanging their energy with the material. Thus the excitation process should be tuned successfully in the stable zones to avoid the degradation of GaAs lifetime.

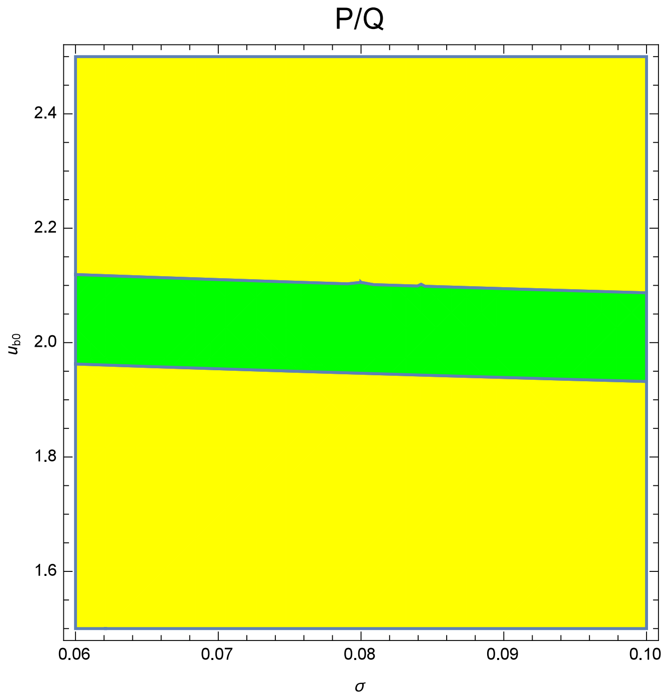

Figure 4. The contour plot for the P/Q ratio where the yellow (green) color represents the region of the unstable (stable) waves. The ratio P/Q depicted against the electron beam velocity u_{b0} and temperature σ with $k = 1$.

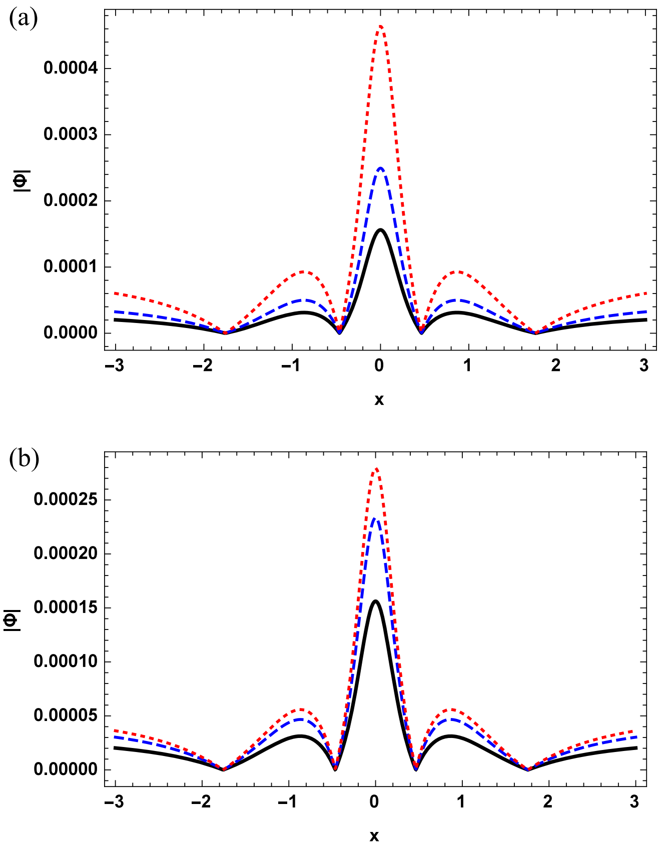

Figure 5. Variation of the rogue wave profile for GaAs. (a) With electron beam velocity $u_{b0} = 3$ (solid curve), $u_{b0} = 3.2$ (dashed curve), and $u_{b0} = 3.5$ (dotted curve) where $\nu = 0.001$, $k = 0.01$, and $\sigma = .06$. (b) With carrier wave number $k = 0.01$ (solid curve), $k = 0.015$ (dashed curve), and $k = 0.1$ (dotted curve) where $\nu = 0.001$, $u_{b0} = 3$, and $\sigma = .06$.

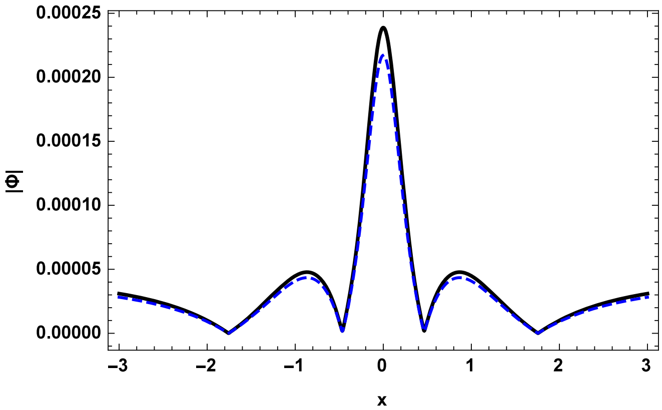

Figure 6. The rogue wave profile for GaAs with Bohm potential effect (solid curve) and without this effect (dashed curve). Here, $\nu = 0.001$, $u_{b0} = 2.45$, $\sigma = .06$, and $k = 0.1$.

5. Conclusions

In this paper, we studied the propagation of solitons, shock-like, and rogue non-linear waves in a system composed of (electron/hole) and pumped by an electron beam. Our model had been applied to GaAs semiconductor plasma that has a great attention for several applications as it characterized by direct energy gap and high carrier mobility. The reductive perturbation method is employed to reduce the basic set of the quantum fluid model to the Korteweg–de Vries (K-dV), modified Korteweg–de Vries (mK-dV), and Gardner equations, which can be transformed into the NLS equation using the modulational instability technique. The results showed that both the electron beam parameters and carrier wave number enhances the generation of several noises that becomes a source of heat and may lead to overheating the GaAs. The analysis of the NLS equation provides us with unstable regions where the rogue waves may be propagated. Moreover, investigation of the quantum effects reveals that the tunneling effect had a significant influence on the pulse profile. Therefore, to increase the lifetime of GaAs one should manage the operation of the electron beam and avoid the perturbed regions which support the generation of these non-linear noises. Eventually, we will build a comparison between our theoretical results and the experimental results of [47] using the PIC electrostatic simulation which provides us with the charge density, current density, and electron temperature. It is convenient also, to investigate other non-linear waves such as breather, blow-up, and soliton rings waves for different types of semiconductor plasma.

Appendix A. The constants of equations (10), (13) and (15)and coefficients of equation (18)

The constants γ_1, γ_2, γ_3, γ_4, and γ_5 and coefficients A, B, and D are given as

$$\gamma_1 = \beta_1 - \left(\frac{-0.985e^2\sqrt[3]{n_{e0}}}{3\in}\right)\left(1 + \frac{0.62458}{1 + 18.37a_{Be}^{*}\sqrt[3]{n_{e0}}}\right),$$

$$\gamma_2 = \beta_2 - \left(\frac{-0.985Me^2\sqrt[3]{n_{h0}}}{3\in}\right)\left(1 + \frac{0.62458}{1 + 18.37a_{Bh}^{*}\sqrt[3]{n_{h0}}}\right),$$

$$\gamma_{3e} = -\left(\frac{-0.985e^2\sqrt[3]{n_{e0}}}{\in}\right),$$

$$\gamma_{3h} = -\left(\frac{-0.985e^2\sqrt[3]{n_{h0}}}{\in}\right),$$

$$\gamma_{4e} = -\left(\frac{-0.985e^2\sqrt[3]{n_{e0}}}{\in}\right)\frac{0.034}{a_{Be}^{*}},$$

$$\gamma_{4h} = -\left(\frac{-0.985e^2\sqrt[3]{n_{h0}}}{\in}\right)\frac{0.034}{a_{Bh}^{*}},$$

$$\gamma_{5e} = \frac{18.37a^*_{Be}}{3(1 + 18.37a^*_{Be}\sqrt[3]{n_{e0}})},$$

$$\gamma_{5h} = \frac{18.37a^*_{Be}}{3(1 + 18.37a^*_{Bh}\sqrt[3]{n_{h0}})},$$

$$A = \left(\frac{2\lambda}{(\beta_1 - \lambda^2)^2} + \frac{2\lambda M\rho}{(\beta_2 - \lambda^2)^2} + \frac{2\mu\nu(u_{b0} - \lambda)}{(3\mu\sigma - (u_{b0} - \lambda)^2)^2}\right)^{-1},$$

$$B = -\frac{27\lambda^2 - 3\beta_1 - 9\gamma_{4e}\gamma_{5e}^2 - 2\gamma_{3e} - 6\gamma_{4e}\gamma_{5e}}{9(\gamma_1 - \lambda^2)^3} + \frac{M^2\rho(-9\beta - 27\lambda^2 + 9\gamma_{4h}\gamma_{5h}^2M + 2\gamma_{3h}M + 6\gamma_{4h}\gamma_{5h}M)}{9(\gamma_2 - \lambda^2)^3} + \frac{3\mu^2\nu(\mu\sigma + (u_{b0} - \lambda)^2)}{(3\mu\sigma - (u_{b0} - \lambda)^2)^3},$$

$$D = \frac{1}{3}\left(3 + \frac{H_e^2}{2(\beta_1 - \lambda^2)^2} + \frac{M\rho H_h^2}{2(\beta_2 - \lambda^2)^2}\right).$$

Appendix B. The derivation of modified Korteweg–de Vries (mK-dV) and Gardner equations

We suggested the following expansion and stretched space-time variables in order to overcome the failure of the (KdV) equation at the critical value of the non-linear term ($B = 0$)

$$\vartheta = \vartheta_0 + \sum_{i=1}^{\infty} \varepsilon^i \vartheta_i, \tag{B1}$$

where $\vartheta_i = [n_e u_e n_b u_b n_h u_h \varphi]^T$ and $\vartheta_0 = [1\ 0\ 1\ u_{b0}\ 1\ 0\ 0]^T$.

$$\xi = \varepsilon(x - \lambda t) \quad \text{and} \quad \tau = \varepsilon^3 t, \tag{B2}$$

Substituting equations (B1) and (B2) into the basic equations (1)–(7) the lowest order in ε gives the last linearized solutions and the compatibility condition while the next-order in ε, yields

$$n_{e2} = \frac{(9\gamma_{4e}\gamma_{5e}^2 + 2\gamma_{3e} + 6\gamma_{4e}\gamma_{5e} + 3\beta_1 - 27\lambda^2)\varphi_1^2}{18(\gamma_1 - \lambda^2)^3} + \frac{\varphi_2}{\gamma_1 - \lambda^2}, \tag{B3}$$

$$n_{h2} = \frac{M^2(3\beta_1 - 27\lambda^2 + 9\gamma_{4h}\gamma_{5h}^2M + 2\gamma_{3h}M + 6\gamma_{4h}\gamma_{5h}M)\varphi_1^2}{18(\gamma_2 - \lambda^2)^3} - \frac{M\varphi_2}{\gamma_2 - \lambda^2}, \tag{B4}$$

$$n_{b2} = -\frac{3\mu^2(\mu\sigma + (u_{b0} - \lambda)^2)\varphi_1^2}{2(3\mu\sigma - (u_{b0} - \lambda)^2)^3} + \frac{\mu\varphi_2}{3\mu\sigma - (u_{b0} - \lambda)^2}, \tag{B5}$$

$$u_{e2} = \frac{(9\gamma_{4e}\gamma_{5e}^2\lambda - 4\gamma_{3e}\lambda - 12\gamma_{4e}\gamma_{5e}\lambda - 15\beta_1\lambda - 9\lambda^3)\varphi_1^2}{18(\gamma_1 - \lambda^2)^3} + \frac{3\lambda\varphi_2}{\gamma_1 - \lambda^2}, \tag{B6}$$

$$u_{h2} = -\frac{\lambda M^2(-15\beta_2 + 9\lambda^2 - 9\gamma_{4h}\gamma_{5h}^2M + 4\gamma_{3h}M + 12\gamma_{4h}\gamma_{5h}M)\varphi_1^2}{18(\gamma_2 - \lambda^2)^3} - \frac{3\lambda M\varphi_2}{\gamma_2 - \lambda^2}, \tag{B7}$$

$$u_{b2} = \frac{\mu^2(u_{b0} - \lambda)(9\mu\sigma + (u_{b0} - \lambda)^2)\varphi_1^2}{2(3\mu\sigma - (u_{b0} - \lambda)^2)^3} + \frac{\mu(\lambda - u_{b0})\varphi_2}{3\mu\sigma - (u_{b0} - \lambda)^2}, \tag{B8}$$

Moreover, the Poisson equation gives

$$\left(\frac{1}{\gamma_1 - \lambda^2} + \frac{\mu\nu}{3\mu\sigma - (u_{b0} - \lambda)^2} + \frac{M\rho}{\gamma_2 - \lambda^2}\right)\varphi_2 = \frac{-1}{2}\left(-\frac{27\lambda^2 - 3\beta_1 - 9\gamma_{4e}\gamma_{5e}^2 - 2\gamma_{3e} - 6\gamma_{4e}\gamma_{5e}}{9(\gamma_1 - \lambda^2)^3} + \frac{3\mu^2\nu(\mu\sigma + (u_{b0} - \lambda)^2)}{(3\mu\sigma - (u_{b0} - \lambda)^2)^3} + \frac{M^2\rho(-9\beta - 27\lambda^2 + 9\gamma_{4h}\gamma_{5h}^2M + 2\gamma_{3h}M + 6\gamma_{4h}\gamma_{5h}M)}{9(\gamma_2 - \lambda^2)^3}\right)\varphi_1^2, \tag{B9}$$

It is clear from equation (B9) that, the coefficient of φ_2 describes the compatibility condition (11), whereas the coefficient of φ_1^2 is identically B which vanishes here. The next-order in ε can be presented by the following equations

$$\frac{\partial n_{e1}}{\partial \tau} - \lambda\frac{\partial n_{e3}}{\partial \xi} + \frac{\partial u_{e3}}{\partial \xi} + \frac{\partial}{\partial \xi}(u_{e1}n_{e2}) + \frac{\partial}{\partial \xi}(u_{e2}n_{e1}) = 0, \tag{B10}$$

$$\frac{\partial u_{e1}}{\partial \tau} - \gamma_{4e}\gamma_{5e}^{2}n_{e2}\frac{\partial n_{e1}}{\partial \xi} - \gamma_{4e}\gamma_{5e}^{2}n_{e1}\frac{\partial n_{e2}}{\partial \xi} - \frac{2}{3}\gamma_{4e}\gamma_{5e}\frac{\partial (n_{e1}n_{e2})}{\partial \xi} - \frac{2}{9}\gamma_{3e}\frac{\partial (n_{e1}n_{e2})}{\partial \xi} - \frac{1}{3}\beta_{1}\frac{\partial (n_{e1}n_{e2})}{\partial \xi}$$
$$+u_{e1}\frac{\partial u_{e2}}{\partial \xi} + u_{e2}\frac{\partial u_{e1}}{\partial \xi} - \gamma_{4e}\gamma_{5e}^{2}n_{e1}^{2}\frac{\partial n_{e1}}{\partial \xi} + \gamma_{4e}\gamma_{5e}\frac{\partial n_{e3}}{\partial \xi} + \frac{1}{3}\gamma_{3e}\frac{\partial n_{e3}}{\partial \xi} + \beta_{1}\frac{\partial n_{e3}}{\partial \xi}$$
$$-\lambda\frac{\partial u_{e3}}{\partial \xi} - \frac{\partial \varphi_{3}}{\partial \xi} + \frac{1}{6}H_{e}^{2}\frac{\partial^{3} n_{e1}}{\partial \xi^{3}} = 0, \tag{B11}$$

$$\frac{\partial n_{h1}}{\partial \tau} - \lambda\frac{\partial n_{h3}}{\partial \xi} + \frac{\partial u_{h3}}{\partial \xi} + \frac{\partial}{\partial \xi}(u_{h1}n_{h2}) + \frac{\partial}{\partial \xi}(u_{h2}n_{h1}) = 0, \tag{B12}$$

$$\frac{\partial u_{h1}}{\partial \tau} - \gamma_{4h}\gamma_{5h}^{2}Mn_{h2}\frac{\partial n_{h1}}{\partial \xi} - \gamma_{4h}\gamma_{5h}^{2}Mn_{h1}\frac{\partial n_{h2}}{\partial \xi} - \frac{2}{3}\gamma_{4h}\gamma_{5h}M\frac{\partial (n_{h1}n_{h2})}{\partial \xi}$$
$$+ \frac{2}{9}\beta_{2}n_{h1}^{2}\frac{\partial n_{h1}}{\partial \xi} - \frac{2}{9}\gamma_{3h}M\frac{\partial (n_{h1}n_{h2})}{\partial \xi} - \frac{1}{3}\beta_{2}\frac{\partial (n_{h1}n_{h2})}{\partial \xi} + u_{h1}\frac{\partial u_{h2}}{\partial \xi} + u_{h2}\frac{\partial u_{h1}}{\partial \xi}$$
$$- M\gamma_{4h}\gamma_{5h}^{2}n_{h1}^{2}\frac{\partial n_{h1}}{\partial \xi} + \gamma_{4h}\gamma_{5h}M\frac{\partial n_{h3}}{\partial \xi} + \frac{1}{3}\gamma_{3h}M\frac{\partial n_{h3}}{\partial \xi}$$
$$+ \beta_{2}\frac{\partial n_{h3}}{\partial \xi} - \lambda\frac{\partial u_{h3}}{\partial \xi} + M\frac{\partial \varphi_{3}}{\partial \xi} + \frac{1}{6}H_{h}^{2}\frac{\partial^{3} n_{h1}}{\partial \xi^{3}} = 0, \tag{B13}$$

$$\frac{\partial n_{b1}}{\partial \tau} + (u_{b0} - \lambda)\frac{\partial n_{b3}}{\partial \xi} + \frac{\partial u_{b3}}{\partial \xi} + \frac{\partial}{\partial \xi}(u_{b1}n_{b2}) + \frac{\partial}{\partial \xi}(u_{b2}n_{b1}) = 0, \tag{B14}$$

$$\frac{\partial u_{b1}}{\partial \tau} + (u_{b0} - \lambda)\frac{\partial u_{b3}}{\partial \xi} + 3\mu\sigma\frac{\partial (n_{b1}n_{b2})}{\partial \xi} + \frac{\partial (u_{b1}u_{b2})}{\partial \xi} + 3\mu\sigma\frac{\partial n_{b3}}{\partial \xi} - \mu\frac{\partial \varphi_{3}}{\partial \xi} = 0, \tag{B15}$$

$$\frac{\partial^{2} \varphi_{1}}{\partial \xi^{2}} - n_{e3} - \nu n_{b3} + \rho n_{h3} = 0. \tag{B16}$$

Therefore, solving the last system of equations with the aid of equations (10) and (B3)–(B8), we obtain a modified Korteweg–de Vries (mK-dV) equation:

$$\frac{\partial \varphi_{1}}{\partial \tau} + AC\ \varphi_{1}^{2}\frac{\partial \varphi_{1}}{\partial \xi} + A\ D\frac{\partial^{3} \varphi_{1}}{\partial \xi^{3}} = 0, \tag{B17}$$

On the other hand, we need to investigate the evolution equation of the system in the vicinity of the critical density(i.e $B \sim O(\varepsilon)$). To do that, we employed the Watanabe method (see [49]) and after some straightforward algebra we get the Gardner equation

$$\frac{\partial \varphi_{1}}{\partial \tau} + (AB\varphi_{1} + AC\ \varphi_{1}^{2})\frac{\partial \varphi_{1}}{\partial \xi} + AD\frac{\partial^{3} \varphi_{1}}{\partial \xi^{3}} = 0. \tag{B18}$$

Where C is the non-linear coefficient and is given as

$$C = \left(\begin{array}{c} -\dfrac{3(9\gamma_{5e}^{2}(9\gamma_{5e}(\gamma_{5e}+2)+4)\gamma_{4e}^{2} + 6\gamma_{5e}(9\gamma_{5e}+4)\gamma_{3e}\gamma_{4e} + 4\gamma_{3e}^{2}) + 4(3\gamma_{5e}\gamma_{4e}(9\gamma_{5e}(2-15\lambda^{2})+4) + 4\gamma_{3e}) + 1215\lambda^{4} + 348\lambda^{2} - 4}{54(\gamma_{1}-\lambda^{2})^{5}} \\ +\dfrac{M^{3}\rho(3(-4M^{2}\gamma_{3e}^{2} + 27\lambda^{2}(20M\gamma_{5e}^{2}\gamma_{4e} + 3\beta_{2}) - 6M\gamma_{3e}(M\gamma_{5e}(9\gamma_{5e}+4)\gamma_{4e} + \beta_{2})))}{54(\gamma_{2}-\lambda^{2})^{5}} \\ +\dfrac{3M^{3}\rho(-9M\gamma_{5e}\gamma_{4e}(M\gamma_{5e}(9\gamma_{5e}(\gamma_{5e}+2)+4)\gamma_{4e} + \beta_{2}(3\gamma_{5e}+2)) - 405\lambda^{4})}{54(\gamma_{2}-\lambda^{2})^{5}} \\ +\dfrac{M^{3}\rho(-2Q(M(3\gamma_{5e}(27\gamma_{5e}+2)\gamma_{4e} + 2\gamma_{3e}) + 9\beta_{2} + 255\lambda^{2}) + 36\beta_{2}^{2})}{54(\gamma_{2}-\lambda^{2})^{5}} \\ +\dfrac{3\nu(\mu^{3}(9\mu^{2}\sigma^{2} + 30\mu\sigma(u_{b0}-\lambda)^{2} + 5(u_{b0}-\lambda)^{4}))}{2((u_{b0}-\lambda)^{2} - 3\mu\sigma)^{5}} \end{array}\right) \tag{B19}$$

ORCID iDs

M S Afify https://orcid.org/0000-0002-2088-0354

References

[1] Yacobi B G 2004 *Semiconductor Materials, An Introduction to Basic Principles* (New York: Kluwer Academic Publishers)
[2] Haug H and Koch S W 2004 *Quantum Theory of the Optical and Electronic Properties of Semiconductors* (United States of America: World Scientific Publishing)
[3] Colak S, Fitzpatrick B J and Bhargava R N 1985 *J. Crystal Growth* **72** 504 and references therein.

[4] Giancoli D C 2008 *Physics for Scientists and Engineers with Modern Physics* (United States of America: Pearson Education)
[5] Voronkov E N 1999 *JETP Lett.* **70** 72
[6] Akimov A V, Scherbakov A V, Yakovlev D R and Bayer M 2015 *Ultrasonics* **56** 122
[7] Ruban V *et al* 2010 *Eur. Phys. J. Spec. Top.* **185** 5
[8] Chen F F 2016 *Introduction to Plasma Physics and Controlled Fusion* (New York: Springer)
[9] Kharif C, Pelinovsky E and Slunyaev A 2009 *Rogue Waves in the Ocean* (Heidelberg: Springer)
[10] Kibler B *et al* 2010 *Nat. Phys. (Lond.)* **6** 790
[11] Akhmediev N and Ankiewicz A 2009 *Phys. Lett.* A **373** 2137
[12] Bludov Y V, Konotop V V and Akhmediev N 2009 *Phys. Rev.* A **80** 033610
[13] Bailung H, Sharma S K and Nakamura Y 2011 *Phys. Rev. Lett.* **107** 255005
[14] Tolba R E, Moslem W M, El-Bedwehy N A and El-Labany S K 2015 *Phys. Plasmas* **22** 043707
[15] Guo S, Mei L, He Y and Li Y 2016 *Phys. Lett.* A **380** 1031
[16] Abd El-Razek H N and Rizk I M 2016 *Int. J. Sci. Res. Sci., Eng. Technol.* **2** 363
[17] Yahia M E, Tolba R E, El-Labany S K, El-Bedwehy N A and Moslem W M 2015 *Sci. Rep.* **5** 12245
[18] El-Bedwehy N A 2014 *Physica* B **442** 114
[19] Gurskii A L, Lutsenko E V, Mitcovets A I and Yablonskii G P 1993 *Physica* B **185** 505
[20] Seeger K 2004 *Semiconductor Physics* (Berlin: Springer)
[21] Shukla P K and Eliasson B 2011 *Rev. Mod. Phys.* **83** 885
[22] Ghorui M K, Chatterjee P and Roychoudhury R 2013 *Indian J Phys.* **87** 77
[23] Yahia M E, Azzouz I M and Moslem W M 2013 *Appl. Phys. Lett.* **103** 082105
[24] El-Said A S, Moslem W M and Djebli M 2014 *Appl. Phys. Lett.* **104** 231609
[25] Hussain S and Akhtar N 2016 *Phys. Plasmas* **23** 092110
[26] Ghosh S and Muley A 2018 *Indian J. Phys.* **92** 121
[27] Hosen B, Shah M G, Hossen M R and Mamun A A 2018 *Plasma Phys. Rep.* **44** 976
[28] El-Tantawy S A, Shan S A, Akhtar N and Elgendy A T 2018 *Chaos Soliton Fract* **113** 356–64
[29] Hussain S and Mahmood S 2018 *Chaos Soliton Fract* **106** 266
[30] Haas F 2019 *Plasma Phys Control Fusion* **61** 044001
[31] Afify M S, Moslem W M and Hassouba M A 2019 *Chaos Soliton Fract* **124** 18–25
[32] Hohenberg P and Kohn W 1964 *Phys. Rev.* **136** 864
[33] Kohn W and Sham L J 1965 *Phys. Rev.* **140** 1133
[34] Yan J, Jacobsen K W and Thygesen K S 2012 *Phys. Rev.* B **86** 241404
[35] Runge E and Gross E K U 1984 *Phys. Rev. Lett.* **52** 997
[36] Marquez M A L 2006 *Time-Dependent Density Functional Theory, Lecture Notes in Physics* (Berlin: Springer)
[37] Brey L, Dempsey J, Johnsen N F and Halperin B I 1990 *Phys. Rev.* B **42** 1240
[38] Crouseilles N, Hervieux P-A and Manfredi G 2008 *Phys. Rev.* B **78** 155412
[39] Choudhury S, Das T K, Ghorui M K and Chatterjee P 2017 *Phys. Plasmas* **24** 062103
[40] Afify M S, Moslem W M, Hassouba M A and Abu-El Hassan A 2018 *Phys. Plasmas* **25** 052116
[41] Chandrasekhar S 1935 *Mon. Not. R. Astron. Soc.* **170** 405
[42] Akbari-Moghanjoughi M 2015 *Phys. Plasmas* **22** 022103
[43] Washimi H and Taniuti T 1966 *Phys. Rev. Lett.* **17** 996
[44] Ur-Rehman H and Mahmood S 2016 *Astrophys Space Sci.* **361** 292
[45] Coelho S M M, Auret F D, Janse van Rensburg P J and Nel J M 2013 *J. Appl. Phys.* **114** 173708
[46] Archilla J F, Jiménez N, Sánchez-Morcillo V J and Garcia-Raffi 2015 *Quodons in Mica: Non-linear Localized Travelling Excitations in Crystals* (Berlin: Springer)
[47] Tunhuma S M, Auret F D, Nel J M, Omotoso E, Danga H T, Igumbor E and Diale M 2017 *Nucl. Instrum. Methods, Sect.* B **409** 36
[48] Sunder W A, Barns R L, Kometani T Y, Parsey J M Jr and Laudise R A 1986 *J. Crystal Growth* **78** 9
[49] Watanable S 1984 *J. Phys. Soc. Jpn.* **53** 950
[50] Raadu M A and Chanteur G 1986 *Phys. Scr.* **33** 240
[51] Akhtar N, El-Tantawy S A, Mahmood S, Wazwaz A, Ur-Rehman H and Ur-Rehman A 2019 *Rom. Rep. Phys.* **71** 403
[52] Ruderman M S, Talipova T and Pelinovsky E 2008 *J. Plasma Phys.* **74** 639
[53] Saini N S, Manpreet S and Bains A S 2015 *Phys. Plasmas* **22** 113702
[54] El-Labany S K, El-Bedwehy N A and Abd El-Razek H N 2007 *Phys. Plasmas* **14** 103704
[55] Ankiewicz A, Devine N and Akhmediev N 2009 *Phys. Lett.* A **373** 3997
[56] Hasegawa A 1975 *Nonlinear Effects and Plasma Instabilities* (Berlin: Springer)